Available online at www.sciencedirect.com
SCIENCE DIRECT®
Journal of Sound and Vibration 271 (2004) 773–787
JOURNAL OF SOUND AND VIBRATION
www.elsevier.com/locate/jsvi

Free vibrations of annular sector cantilever plates. Part 2: in-plane motion

Jongwon Seok*, H.F. Tiersten

Department of Mechanical, Aerospace and Nuclear Engineering, Rensselaer Polytechnic Institute, 110 8th Street, Troy, NY 12180-3590, USA

Received 4 June 2002; accepted 12 March 2003

Abstract

Analysis of the free in-plane vibrations of a cantilevered annular sector plate is performed by means of a variational approximation procedure. The problem is treated by first obtaining the exact solution for waves in the plate satisfying the equations of plane stress including in-plane inertia with the inner and outer circumferential edges traction free. In this exact solution, new radial vector functions are obtained from a Fröbenius type expansion. The solution results in a set of dispersion curves. A number of the resulting waves are used in what remains of the variational equation, in which all conditions occur as natural conditions. Roots of the resulting transcendental equation are calculated, which yield the eigensolutions and associated eigenfrequencies. The results are compared with results obtained using FEM, and good agreement is shown.

1. Introduction

In this work, the equations of plane stress are used to treat the problem of the free vibrations of a thin annular sector cantilevered plate. Although the results obtained from the analysis of the transverse vibrations of a thin annular sector plate are available for a range of boundary conditions and aspect ratios, the authors could not find any work on the in-plane motion of the annular sector plate in the open literature. Ambati et al. [1] broadly investigated the in-plane vibrations of complete annular rings. They performed the eigenanalyses of the complete annular rings analytically based on the two wave equations, one is rotational and the other dilatational, and presented the numerical and experimental results with the considerations of the various aspect

*Corresponding author. Tel.: +1-518-276-8003; fax: +1-518-276-8761.
E-mail address: seokj@alum.rpi.edu (J. Seok).

0022-460X/03/$ - see front matter
doi:10.1016/S0022-460X(03)00415-2

ratios of the outer and inner radii and the wide range of Poisson's ratios. However, this work is confined to the study of complete annular rings with free edges. Irie et al. [2] treated the in-plane vibrations of complete annular rings with a variety of aspect ratios of the outer and inner radii and four sets of edge conditions as combinations of free and clamped conditions. This work uses a state vector composed of two in-plane displacements, and normal and shear stress resultants. However, as already noted, no published work was found on in-plane vibrations of the annular sector plate.

In this investigation, the problem of the in-plane vibrations of the annular sector plate is treated, in which the plate is fixed on one radial edge, free on the other and free on both circumferential edges. Since this problem cannot be solved exactly, some form of approximation procedure must be employed. As in Part 1 [3], a variational approximation procedure is used, in which the dynamic differential equations of plane stress and traction-free conditions on the two circumferential edges are satisfied exactly and the remaining free and fixed edge conditions on the radial edges are satisfied variationally. The treatment employs the variational equation of linear elastic plane stress with in-plane inertia, in which all conditions, i.e., those of both natural and constraint types, arise as natural conditions in a form suitable for the application in this work. The required variational equation derived in recent work [4] is in rectilinear co-ordinates, and must be transformed to cylindrical co-ordinates for the application in this work. As in the other work, the analysis proceeds by first obtaining solutions satisfying the dynamic linear plane stress equations and the traction-free conditions on the two circumferential edges exactly. In finding these exact solutions, the radial differential equations arising are not expanded about the usual singular point, but instead are expanded about a regular point, for which the required number of coupled independent radial vectorial power series solutions is always obtained [5]. In this exact solution, new radial vector functions are found by using a Fröbenius type expansion, which are then used to satisfy the circumferential edge conditions of the intermediate problem exactly. The remaining conditions on the two radial edges are then satisfied variationally.

The exact solution of the differential equations and traction-free conditions on the two circumferential edges yields dispersion curves. The dispersion curves for in-plane flexure of annular sector plates presented in this work are exact and, to our knowledge, have not appeared in the literature before. Up to seven of these solutions are taken, which are represented by the dispersion curves, in what remains of the variational equation with all natural conditions to obtain a system of linear homogeneous algebraic equations, from which calculations are performed. Among other things, the calculations clearly show the dependence of the natural frequencies on the radial dimension of the plate for a given circumferential dimension. The results compare favorably with those from P3/PATRAN [6].

2. Variational equation for the in-plane motion of a thin orthotropic plate

In previous work [4], the variational equation for both the extension and flexure of thin plates, in which all conditions, i.e., those of both natural and constraint types, arise as natural conditions was obtained from the appropriate three-dimensional variational equation [7] by expanding the displacement in a sum of powers of the thickness co-ordinate of the plate [8]. The flexural portion of the variational equation derived in Ref. [4] was employed in performing an eigenanalysis for the

flexural vibrations of an annular sector plate having polar orthotropic symmetry in Part 1. In this work, the flexural portion, which uncouples from the extensional portion, is taken to vanish and only the in-plane portion is retained. Accordingly, from Eq. (1) of Ref. [9], the remaining in-plane part of the variational equation can be written in the form

$$\int_{t_0}^{t} \mathrm{d}t \left[\int_S (\tau_{ab,a}^{(0)} - 2\rho h \ddot{u}_b^{(0)}) \delta u_b^{(0)} \mathrm{d}S - \int_{c_N} n_a \tau_{ab}^{(0)} \delta u_b^{(0)} \mathrm{d}s + \int_{c_C} u_b^{(0)} \delta (n_a \tau_{ab}^{(0)}) \mathrm{d}s \right] = 0, \tag{1}$$

in which Hamilton's principle was modified to include not only the edges c_N on which the tractions are prescribed, but also the edges c_C on which the displacements are prescribed by means of the method of Lagrange multipliers [10]. Here, the two-dimensional components of the in-plane stress resultants are defined by

$$\tau_{ab}^{(0)} = \int_{-h}^{h} \tau_{ab} \mathrm{d}x_3 \tag{2a}$$

and the two-dimensional components of the in-plane displacement are defined by the relation

$$u_b = \sum_{n=0}^{1} x_3^n u_b^{(n)}(x_a, t) \tag{2b}$$

and the notation is defined in Section 2 of Part 1. Note that a fixed Cartesian co-ordinate system x_i has been employed, with the faces of the plate of area S, at $x_3 = \pm h$, and the axes x_1 and x_2 in the mid-plane. All of the inhomogeneous terms in Eq. (1) have been ignored since they are not needed in this work.

Now, consider a cylindrical co-ordinate system r, θ, z with unit vectors $\hat{r}, \hat{\theta}, \hat{z}$, as shown in Fig. 1 and in Fig. 1(b) of Part 1. The faces of the plate, of area S, are at $x_3 = z = \pm h$ as shown in Fig. 1. The origin of the cylindrical co-ordinate system is at $r = 0$ and the plate is bounded by a fixed edge at $\theta = -\Theta$ and three free edges at $\theta = \Theta$, $r = R_i, R_o$. As in Part 1, the material of the plate is taken to have polar orthotropic symmetry, in which the three-dimensional extensional constitutive equations are not coupled with the independent shear constitutive equations.

From the assumption of plane stress and with the three-dimensional constitutive equations for the plate having polar orthotropic symmetry, the two-dimensional constitutive equations for the lowest order extensional motion of the plate may, with the aid of the compressed matrix notation given in Table 1 of Part 1, where the tensor indices 1, 2, 3 correspond to r, θ, z, be written in the

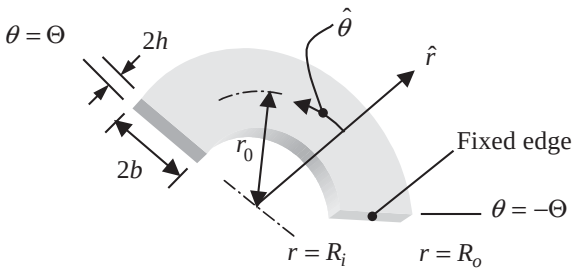

Fig. 1. Three-dimensional view of an annular sector plate fixed on one edge and free on the other three.

form (see Eqs. (2)–(5) of Ref. [9])

$$\tau_{11}^{(0)} = 2hc_{11}^{*}\left(\varepsilon_{11}^{(0)} + \hat{v}\varepsilon_{22}^{(0)}\right), \quad \tau_{22}^{(0)} = 2hc_{11}^{*}\left(R\varepsilon_{22}^{(0)} + \hat{v}\varepsilon_{11}^{(0)}\right), \quad \tau_{12}^{(0)} = 2hc_{66}\cdot 2\varepsilon_{12}^{(0)}, \tag{3}$$

where the infinitesimal strain–displacement gradient relations in polar co-ordinates may be written in the form

$$\varepsilon_{11}^{(0)} = u_{1,1}^{(0)}, \quad \varepsilon_{12}^{(0)} = \frac{\left(u_1^{(0)} + u_{2,2}^{(0)}\right)}{r}, \quad \varepsilon_{12}^{(0)} = \frac{1}{2}\left(\frac{u_{1,2}^{(0)}}{r} + u_{2,1}^{(0)} - \frac{u_2^{(0)}}{r}\right) \tag{4}$$

and the two-dimensional polar orthotropic elastic constants are defined in terms of the three-dimensional polar orthotropic elastic constants by

$$c_{11}^{*} = c_{11} - c_{13}^{2}/c_{33}, \quad c_{12}^{*} = c_{12} - c_{13}c_{32}/c_{33}, \quad c_{22}^{*} = c_{22} - c_{23}^{2}/c_{33}. \tag{5}$$

For later use, the following dimensionless quantities are now defined:

$$\hat{v} = c_{12}^{*}/c_{11}^{*}, \quad R = c_{22}^{*}/c_{11}^{*}. \tag{6}$$

The transformation of the variational equation (1) to the cylindrical co-ordinate system with the aid of the definition of the tensor indices 1, 2, 3 enables us to write

$$\begin{aligned}
&\int_S \mathrm{d}S\left[\left\{\tau_{rr,r}^{(0)} + \frac{\tau_{r\theta,\theta}^{(0)}}{r} + \frac{\left(\tau_{rr}^{(0)} - \tau_{\theta\theta}^{(0)}\right)}{r} - 2\rho h\ddot{u}_r^{(0)}\right\}\delta u_r^{(0)} + \left\{\frac{\tau_{\theta\theta,\theta}^{(0)}}{r} + \tau_{r\theta,r}^{(0)} + \frac{2\tau_{r\theta}^{(0)}}{r} - 2\rho h\ddot{u}_\theta^{(0)}\right\}\delta u_\theta^{(0)}\right] \\
&\quad - \int_{-\Theta}^{\Theta}\left[r\left(\tau_{rr}^{(0)}\delta u_r^{(0)} + \tau_{r\theta}^{(0)}\delta u_\theta^{(0)}\right)\right]_{r=R_i}^{r=R_o}\mathrm{d}\theta - \int_{R_i}^{R_o}\left[\tau_{\theta\theta}^{(0)}\delta u_\theta^{(0)} + \tau_{\theta r}^{(0)}\delta u_r^{(0)}\right]_{\theta=\Theta}\mathrm{d}r \\
&\quad - \int_{R_i}^{R_o}\left[u_\theta^{(0)}\delta\tau_{\theta\theta}^{(0)} + u_r^{(0)}\delta\tau_{\theta r}^{(0)}\right]_{\theta=-\Theta}\mathrm{d}r = 0,
\end{aligned} \tag{7}$$

where the time integration has been omitted since it is not needed in this work, and the definitions

$$[p(x)]_{x=a}^{x=b} = p(b) - p(a), \ \text{ at } \ [p(x)]_{x=q} = p(q) \tag{8}$$

have been employed.

As discussed in Ref. [4], since in the formulation the constraint conditions were included by the method of Lagrange multipliers, each variation is treated as independent, the coefficient of each variation in Eq. (7) must vanish, which yields the differential equations and edge conditions. However, since the resulting equations cannot be solved exactly, the intermediate problem of satisfying the differential equations and edge conditions on the two circumferential edges exactly is treated first. This solution yields dispersion curves giving frequency vs. wavenumber in the θ direction relations. In the next section the dispersion relations for the in-plane motion of the annular sector plate are obtained.

Since $\delta u_r^{(0)}$ and $\delta u_\theta^{(0)}$ in the surface integral in Eq. (7) are independent, the governing differential equations for the in-plane motion of the plate in the cylindrical co-ordinate system are obtained in the form

$$\frac{\partial\tau_{rr}^{(0)}}{\partial r} + \frac{1}{r}\frac{\partial\tau_{r\theta}^{(0)}}{\partial\theta} + \frac{\left(\tau_{rr}^{(0)} - \tau_{\theta\theta}^{(0)}\right)}{r} = 2\rho h\ddot{u}_r^{(0)}, \tag{9}$$

$$\frac{1}{r}\frac{\tau_{\theta\theta}^{(0)}}{\partial\theta}+\frac{\partial\tau_{r\theta}^{(0)}}{\partial r}+\frac{2\tau_{r\theta}^{(0)}}{r}=2\rho h\ddot{u}_{\theta}^{(0)}. \tag{10}$$

Moreover, since the variations $\delta u_r^{(0)}$ and $\delta u_\theta^{(0)}$ at $r=R_i,R_o$ along the traction-free circumferential edges are independent, the two edge conditions

$$\tau_{rr}^{(0)}=0,\quad \tau_{r\theta}^{(0)}=0,\ \text{at}\ r=R_i,R_o \tag{11}$$

are obtained.

The substitution of the two-dimensional strain–displacement gradient relations (4) into the constitutive equation (3) yields the two-dimensional stress resultant–displacement gradient relations

$$\tau_{rr}^{(0)}=2hc_{11}^{*}\left\{\frac{\partial u_r^{(0)}}{\partial r}+\hat{v}\left(\frac{1}{r}\frac{\partial u_\theta^{(0)}}{\partial\theta}+\frac{u_r^{(0)}}{r}\right)\right\}, \tag{12}$$

$$\tau_{r\theta}^{(0)}=2hc_{66}\left\{\frac{1}{r}\frac{\partial u_r^{(0)}}{\partial\theta}+r\frac{\partial}{\partial r}\left(\frac{u_\theta^{(0)}}{r}\right)\right\}, \tag{13}$$

$$\tau_{\theta\theta}^{(0)}=2hc_{11}^{*}\left\{\hat{v}\frac{\partial u_r^{(0)}}{\partial r}+\frac{R}{r}\left(\frac{\partial u_\theta^{(0)}}{\partial\theta}+u_r^{(0)}\right)\right\}. \tag{14}$$

3. Solution of the differential equations and edge conditions on the two traction-free circumferential faces

The substitution of Eqs. (12)–(14) into Eqs. (9) and (10) yields the differential equations for the in-plane motion of the polar orthotropic plate in the form

$$\begin{aligned}&\frac{c_{11}^{*}}{r}\left\{\frac{\partial}{\partial r}\left(r\frac{\partial u_r^{(0)}}{\partial r}\right)-\frac{Ru_r^{(0)}}{r}\right\}\\&\quad+\frac{1}{r}\frac{\partial}{\partial\theta}\left\{\frac{c_{66}}{r}\frac{\partial u_r^{(0)}}{\partial\theta}+(c_{11}^{*}\hat{v}+c_{66})\frac{\partial u_\theta^{(0)}}{\partial r}-(c_{11}^{*}R+c_{66})\frac{u_\theta^{(0)}}{r}\right\}=\rho\ddot{u}_r^{(0)},\end{aligned} \tag{15}$$

$$\begin{aligned}&\frac{1}{r}\frac{\partial}{\partial\theta}\left\{\frac{c_{11}^{*}R}{r}\frac{\partial u_\theta^{(0)}}{\partial\theta}+(c_{11}^{*}\hat{v}+c_{66})\frac{\partial u_r^{(0)}}{\partial r}+(c_{11}^{*}R+c_{66})\frac{u_r^{(0)}}{r}\right\}\\&\quad+\frac{c_{66}}{r}\left\{\frac{\partial}{\partial r}\left(r\frac{\partial u_\theta^{(0)}}{\partial r}\right)-\frac{u_\theta^{(0)}}{r}\right\}=\rho\ddot{u}_\theta^{(0)}.\end{aligned} \tag{16}$$

From Eq. (11), along with Eqs. (12) and (13), the traction-free edge conditions at the two circumferential edges are given by

$$2hc_{11}^{*}\left\{\frac{\partial u_r^{(0)}}{\partial r}+\hat{v}\left(\frac{1}{r}\frac{\partial u_\theta^{(0)}}{\partial\theta}+\frac{u_r^{(0)}}{r}\right)\right\}=0,\ \text{at}\ r=R_i,\ R_o, \tag{17}$$

$$2hc_{66}\left\{\frac{1}{r}\frac{\partial u_r^{(0)}}{\partial\theta}+r\frac{\partial}{\partial r}\left(\frac{u_\theta^{(0)}}{r}\right)\right\}=0,\quad \text{at } r=R_i,\ R_o. \tag{18}$$

As a solution of Eqs. (15) and (16), write

$$u_r^{(0)}=\Re\{F(r)\sin(\zeta\theta)\mathrm{e}^{\mathrm{i}\omega t}\}, \tag{19}$$

$$u_\theta^{(0)}=\Re\{G(r)\cos(\zeta\theta)\mathrm{e}^{\mathrm{i}\omega t}\}, \tag{20}$$

where $\mathrm{i}=\sqrt{-1}$, $F(r)$, $G(r)$ are functions of r to be determined, and the symbol $\Re\{\}$ signifies the real part of the argument and will be dropped hereafter.

Eqs. (19) and (20) satisfy Eqs. (15) and (16), provided

$$c_{11}^*F''+\frac{c_{11}^*}{r}F'+\left(\rho\omega^2-\frac{c_{11}^*R+c_{66}\zeta^2}{r^2}\right)F-(c_{11}^*\hat{v}+c_{66})\frac{\zeta}{r}G'+(c_{11}^*R+c_{66})\frac{\zeta}{r^2}G=0, \tag{21}$$

$$c_{66}G''+\frac{c_{66}}{r}G'+\left(\rho\omega^2-\frac{c_{66}+c_{11}^*R\zeta^2}{r^2}\right)G+(c_{11}^*\hat{v}+c_{66})\frac{\zeta}{r}F'+(c_{11}^*R+c_{66})\frac{\zeta}{r^2}F=0, \tag{22}$$

where the superscript prime ($'$) means the derivative with respect to r. Eqs. (21) and (22) are two coupled second-order linear ordinary differential equations in r. Although they are linear, the coupled differential equations cannot be satisfied with any functions known since they constitute a vector system rather than a scalar system. However, solutions satisfying the coupled equations (21) and (22) may readily be obtained by means of an expansion of both F and G in powers of r, just as for scalar equations. Clearly, the extension is straightforward and in this instance serves to define four independent coupled solutions of Eqs. (21) and (22). Since the existence of the singular point at $r=0$ causes numerous difficulties in the coupled series solutions of Eqs. (21) and (22), we obtain coupled series solutions about a point other than $r=0$, for which it is known [5] that expansion about a regular point of the system of coupled second order differential equations (21) and (22) with variable coefficients yields four independent coupled exact power series solutions about that point, which are well behaved in the region of interest. For the best convergence, we expand about the point r_0 in the center of the annulus. This procedure effectively defines four independent coupled exact radially dependent functions satisfying Eqs. (21) and (22), which are particularly convenient for satisfying the four edge conditions (17) and (18) at the inner and outer radii of the annular sector.

For the purpose of calculation, it is convenient to introduce the dimensionless quantities defined in the form

$$\bar{r}=\pi r/(2b),\quad \bar{r}_0=\pi r_0/(2b),\quad \tilde{r}=\bar{r}-\bar{r}_0, \tag{23}$$

$$\bar{c}_{11}^*=c_{11}^*/c_{66},\quad \bar{\Omega}=\omega/\bar{\omega},\quad \tau=\bar{\omega}t, \tag{24}$$

where r_0, as already noted, denotes the center radius of the annulus and

$$b=\frac{R_o-R_i}{2},\quad \bar{\omega}=\frac{\pi}{2b}\sqrt{\frac{c_{66}}{\rho}}. \tag{25}$$

The substitution of Eqs. (23) and (24) into Eqs. (21) and (22) puts the coupled differential equations in the form

$$\bar{c}_{11}^{*}(\tilde{r}+\bar{r}_0)^2F''+\bar{c}_{11}^{*}(\tilde{r}+\bar{r}_0)F'+\left\{\bar{\Omega}^2(\tilde{r}+\bar{r}_0)^2-(\bar{c}_{11}^{*}R+\zeta^2)\right\}F$$
$$-(\bar{c}_{11}^{*}\hat{v}+1)\zeta(\tilde{r}+\bar{r}_0)G'+(\bar{c}_{11}^{*}R+1)\zeta G=0, \tag{26}$$

$$(\tilde{r}+\bar{r}_0)^2G''+(\tilde{r}+\bar{r}_0)G'+\{\bar{\Omega}^2(\tilde{r}+\bar{r}_0)^2-(1+\bar{c}_{11}^{*}R\zeta^2)\}G$$
$$+(\bar{c}_{11}^{*}\hat{v}+1)\zeta(\tilde{r}+\bar{r}_0)F'+(\bar{c}_{11}^{*}R+1)\zeta F=0, \tag{27}$$

where the superscript prime ($'$) means the derivative with respect to the dimensionless radius $\tilde{r}$.

Four coupled independent solutions of Eqs. (26) and (27) are now sought in order to satisfy the four edge conditions given in Eqs. (17) and (18). The most convenient way of obtaining the four independent solutions is to introduce the Fröbenius form [11]

$$F(\tilde{r};\bar{\Omega},\zeta)=\sum_{m=0}^{M}\bar{\alpha}_m\tilde{r}^{\lambda+m},\quad G(\tilde{r};\bar{\Omega},\zeta)=\sum_{m=0}^{M}\bar{\beta}_m\tilde{r}^{\lambda+m}, \tag{28, 29}$$

where $\bar{\alpha}_m(\lambda;\bar{\Omega},\zeta)$ and $\bar{\beta}_m(\lambda;\bar{\Omega},\zeta)$ are respectively the coefficients of $\tilde{r}^{\lambda+m}$ for the function F and G, and $M+1$ is the number of terms in those power series required for convergence. It should also be noticed that in the above equations the functions $F(r), G(r)$ defined in Eqs. (19) and (20) have been replaced by new functions $F(\tilde{r}), G(\tilde{r})$, respectively, which for corresponding points r and $\tilde{r}$ have the same values as the former functions and for the sake of convenience are denoted by the same symbols. This simplification is to be understood in this work.

The substitution of Eqs. (28) and (29) into Eqs. (26) and (27) and the collection of the coefficients of like powers of $\tilde{r}$ in each equation yields the coupled recursion relations for all the solutions, which are much too cumbersome to include, and the coefficients of $\tilde{r}^{\lambda-2}$, which is the lowest power term in each of Eqs. (26) and (27), yield the respective indicial equations in the form

$$\bar{\alpha}_0\bar{c}_{11}^{*}\bar{r}_0\lambda(\lambda-1)=0,\quad \bar{\beta}_0\bar{r}_0\lambda(\lambda-1)=0, \tag{30a, b}$$

which indicate that for $\lambda=0$ and $\lambda=1$, there are four independent solutions, which may be selected in the particularly convenient form, in which the first terms are uncoupled, i.e., one with $\bar{\alpha}_0=1$, $\bar{\beta}_0=0$ and the other with $\bar{\alpha}_0=0$, $\bar{\beta}_0=1$. The integer M is determined by a direct comparison of the coefficients of each power of $\tilde{r}$ until convergence is obtained. Accordingly, the four independent sets of solutions may be denoted by

$$f_1=\sum_{m=0}^{M}\bar{\alpha}_m^{(1)}\tilde{r}^m,\quad g_1=\sum_{m=0}^{M}\bar{\beta}_m^{(1)}\tilde{r}^m, \tag{31a}$$

$$f_2=\sum_{m=0}^{M}\bar{\alpha}_m^{(2)}\tilde{r}^m,\quad g_2=\sum_{m=0}^{M}\bar{\beta}_m^{(2)}\tilde{r}^m \tag{31b}$$

$$f_3=\sum_{m=0}^{M}\bar{\alpha}_m^{(3)}\tilde{r}^{1+m},\quad g_3=\sum_{m=0}^{M}\bar{\beta}_m^{(3)}\tilde{r}^{1+m} \tag{31c}$$

$$f_4=\sum_{m=0}^{M}\bar{\alpha}_m^{(4)}\tilde{r}^{1+m},\quad g_4=\sum_{m=0}^{M}\bar{\beta}_m^{(4)}\tilde{r}^{1+m}, \tag{31d}$$

where the $\bar{\alpha}_m^{(q)}$ and $\bar{\beta}_m^{(q)}$ $(q = 1, \ldots, 4)$ are determined from the coupled recursion equations in accordance with the scheme defined by

$$\bar{\alpha}_m^{(1)}, \quad \bar{\beta}_m^{(1)} \sim \bar{\alpha}_0 = 1, \quad \bar{\beta}_0 = 0 \text{ with } \lambda = 0, \tag{32a}$$

$$\bar{\alpha}_m^{(2)}, \quad \bar{\beta}_m^{(2)} \sim \bar{\alpha}_0 = 0, \quad \bar{\beta}_0 = 1 \text{ with } \lambda = 0, \tag{32b}$$

$$\bar{\alpha}_m^{(3)}, \quad \bar{\beta}_m^{(3)} \sim \bar{\alpha}_0 = 1, \quad \bar{\beta}_0 = 0 \text{ with } \lambda = 1, \tag{32c}$$

$$\bar{\alpha}_m^{(4)}, \quad \bar{\beta}_m^{(4)} \sim \bar{\alpha}_0 = 0, \quad \bar{\beta}_0 = 1 \text{ with } \lambda = 1. \tag{32d}$$

From Eqs. (17) and (18) along with Eqs. (19) and (20), and the introduction of the dimensionless variables defined in Eqs. (23)–(25), the four edge conditions may be written in the dimensionless form

$$F' - \frac{\hat{v}}{\bar{r}_0 + \tilde{r}}(\zeta G - F) = 0, \text{ at } \tilde{r} = \pm\pi/2, \tag{33}$$

$$G' + \frac{1}{\bar{r}_0 + \tilde{r}}(\zeta F - G) = 0, \text{ at } \tilde{r} = \pm\pi/2. \tag{34}$$

In accordance with the foregoing, the solutions of Eqs. (33) and (34) may be written in the form

$$F = \sum_{q=1}^{4} A_q f_q, \quad G = \sum_{q=1}^{4} A_q g_q. \tag{35}$$

The substitution of the coupled solutions equations (35) into Eqs. (33) and (34) yields four homogeneous equations with four unknowns A_q, which can be written in the form

$$\sum_{q=1}^{4}\left[\left\{f_q' - \frac{\hat{v}}{\bar{r}_0 + \tilde{r}}(\zeta g_q - f_q)\right\}A_q\right] = 0, \text{ at } \tilde{r} = \pm\pi/2, \tag{36}$$

$$\sum_{q=1}^{4}\left[\left\{g_q' + \frac{1}{\bar{r}_0 + \tilde{r}}(\zeta f_q - g_q)\right\}A_q\right] = 0, \text{ at } \tilde{r} = \pm\pi/2, \tag{37}$$

which may be written in the convenient algebraic form

$$\sum_{q=1}^{4} L_{pq} A_q = 0, \quad p = 1, \ldots, 4, \tag{38}$$

where $p = 1, 2$ refers to the two edge conditions in Eq. (36) and $p = 3, 4$ refers to the two edge conditions in Eq. (37). Clearly, in matrix notation, Eq. (38) may be written in the form

$$\mathbf{LA} = \mathbf{0}. \tag{39}$$

The vanishing of the determinant of $\mathbf{L}$ in Eq. (39) gives the dispersion relations, and the amplitude ratios for any solution point on the dispersion curves may be obtained from any three of the consistent homogeneous equations in Eq. (39).

The cut-off frequencies, i.e., the non-zero frequencies for $\zeta = 0$, provide good starting points for almost all of the real and imaginary branches of the dispersion curves. When $\zeta = 0$, the coupled

equations (21) and (22) simplify considerably and it is of interest to note that they can be written in the uncoupled form

$$\frac{\mathrm{d}^2F(\xi)}{\mathrm{d}\xi^2}+\frac{1}{\xi}\frac{\mathrm{d}F(\xi)}{\mathrm{d}\xi}+\left(1-\frac{R}{\xi^2}\right)F(\xi)=0, \tag{40}$$

$$\frac{\mathrm{d}^2G(\eta)}{\mathrm{d}\eta^2}+\frac{1}{\eta}\frac{\mathrm{d}G(\eta)}{\mathrm{d}\eta}+\left(1-\frac{1}{\eta^2}\right)G(\eta)=0, \tag{41}$$

which clearly constitute two Bessel differential equations. We now note that the independent dimensionless variables, ξ and η in Eqs. (40) and (41), are given by

$$\xi=\bar{\Omega}(\tilde{r}+\bar{r}_0)/\sqrt{\bar{c}^*_{11}},\quad \eta=\bar{\Omega}(\tilde{r}+\bar{r}_0). \tag{42}$$

In addition, for $\zeta=0$ the traction-free circumferential edge conditions (17) and (18) also become uncoupled, thus

$$\frac{\mathrm{d}F}{\mathrm{d}\tilde{r}}+\frac{\hat{\nu}F}{(\tilde{r}+\bar{r}_0)}=0,\quad \text{at } \tilde{r}=\pm\frac{\pi}{2}, \tag{43}$$

$$\frac{\mathrm{d}G}{\mathrm{d}\tilde{r}}-\frac{G}{(\tilde{r}+\bar{r}_0)}=0,\quad \text{at } \tilde{r}=\pm\frac{\pi}{2}. \tag{44}$$

On account of these simplifications, we write the solutions for $\zeta=0$ in the usual way, thus

$$F(\tilde{r})=C_1\mathrm{J}_{\sqrt{R}}\left\{\bar{\Omega}(\tilde{r}+\bar{r}_0)/\sqrt{\bar{c}^*_{11}}\right\}+C_2\mathrm{Y}_{\sqrt{R}}\left\{\bar{\Omega}(\tilde{r}+\bar{r}_0)/\sqrt{\bar{c}^*_{11}}\right\}, \tag{45}$$

$$G(\tilde{r})=D_1\mathrm{J}_1\{\bar{\Omega}(\tilde{r}+\bar{r}_0)\}+D_2\mathrm{Y}_1\{\bar{\Omega}(\tilde{r}+\bar{r}_0)\}, \tag{46}$$

where in accordance with convention J and Y denote Bessel functions of the first and second kind and $C_n,\ D_n,\ n=1,2$ are arbitrary constants. The substitution of Eqs. (45) and (46) into Eqs. (43) and (44), respectively, yields two independent sets of equations, each of which consist of two homogeneous linear algebraic equations with two unknowns, which for non-trivial solutions yields two sets of cut-off frequencies. For later use, note that for the transversely isotropic material,[1] there results

$$\bar{c}^*_{11}=2/(1-\hat{\nu}). \tag{47}$$

Note further that even for the isotropic case, four independent solutions of Eqs. (26) and (27) are always obtained as indicated in Eqs. (30)–(32), which insures the satisfaction of the four circumferential edge conditions in Eqs. (33) and (34).

It should be noted that since two dimensions are required to locate the circumferential portions of the annular sector plate, the dispersion curves depend on a dimensional ratio in addition to the effective Poisson's ratio $\hat{\nu}$. Since the differential equations and circumferential homogeneous edge conditions are satisfied exactly, the satisfaction of the remaining radial edge conditions variationally yields the result. This will be explained in more detail in the next section. One of the advantages of this approach is the small size of the remaining equation.

[1] The analysis is performed for a polar orthotropic material because the solution for that symmetry is required in future work.

4. Variational approximation

Since the solution functions (35) satisfy the coupled differential equations (26) and (27) and the circumferential edge conditions (33) and (34) exactly, all that remains in the variational equation (7) is

$$-\int_{R_i}^{R_o} \mathrm{d}r\left[\left[u_\theta^{(0)}\delta\tau_{\theta\theta}^{(0)}+u_r^{(0)}\delta\tau_{\theta r}^{(0)}\right]_{\theta=-\Theta}+\left[\tau_{\theta\theta}^{(0)}\delta u_\theta^{(0)}+\tau_{\theta r}^{(0)}\delta u_r^{(0)}\right]_{\theta=\Theta}\right]=0. \tag{48}$$

From Eqs. (19), (20) and (35), when P dispersion curves are included, it is clear that the solution may be written in the form

$$u_r^{(0)}(\tilde{r},\theta,\tau)=\sum_{p=1}^{P}\sum_{q=1}^{4}\sum_{n=1}^{2}B_{pn}\bar{A}_{pq}f_q^{(p)}\sin\{\zeta_p\theta+(n-1)\pi/2\}\mathrm{e}^{\mathrm{i}\bar{\Omega}\tau}, \tag{49}$$

$$u_\theta^{(0)}(\tilde{r},\theta,\tau)=\sum_{p=1}^{P}\sum_{q=1}^{4}\sum_{n=1}^{2}B_{pn}\bar{A}_{pq}g_q^{(p)}\cos\{\zeta_p\theta+(n-1)\pi/2\}\mathrm{e}^{\mathrm{i}\bar{\Omega}\tau}, \tag{50}$$

where the B_{pn} are arbitrary constants and

$$\bar{A}_{pq}=\bar{A}_q(\zeta_p),\quad f_q^{(p)}=f_q(\zeta_p),\quad g_q^{(p)}=g_q(\zeta_p). \tag{51}$$

When the solution functions in Eqs. (49) and (50) are inserted in the variational equation (48), the resulting linear algebra uncouples into two distinct sets of linear homogeneous equations. The transcendental equations that arise when the determinant resulting from each of the uncoupled homogeneous linear algebras vanishes yield the same eigenfrequencies, which by comparison with a PATRAN calculation is the correct frequency in each case. Consequently, a double root is always obtained from the variational equation (48). On account of this the amplitude ratios between the two uncoupled eigensolutions cannot be determined uniquely from this description.[2] Clearly, this particular algebraic difficulty is caused by the use of the same functional behavior in both the solution functions and the variations for the particular conditions for the cantilever, in which one edge has displacement conditions going through the variation in traction and the other edge has traction conditions going through the variation in displacement, as shown in Eq. (48).[3] Although this non-uniqueness of the amplitude ratios can be tolerated and would be removed if a forced vibration problem were treated, since it is unusual and only free vibration problems are treated in this work, it seems preferable to remove the double root and associated non-uniqueness of the amplitude ratios from the free vibration description. To this end an auxiliary constraint

[2] The discussion in the text is for the case when the origin of co-ordinates is at the center of the cantilever, which is when the complete decoupling into two distinct sets of linear homogeneous equations occurs. If the origin is placed other than at the center of the cantilever, one set of linear homogeneous algebraic equations is obtained, but the resulting determinant does not exhibit a zero crossing and has a horizontal slope at the root, which does not yield the eigenfrequencies as accurately as when a zero crossing exists. In addition, at the eigenfrequencies the rank of the apparently fully coupled matrix is reduced by two [13] and two distinct algebraic solutions are still obtained and the amplitude ratios are not unique.

[3] Exactly the same thing happens in the case of a cantilever beam, for which an exact solution can readily be obtained, in which the amplitude ratios are uniquely determined. If the edge conditions for the beam are satisfied variationally, a double root is obtained and the amplitude ratios cannot be uniquely determined.

condition is introduced at the fixed edge. The mean radial displacement is taken to vanish as the constraint condition, which is introduced in the variational equation (48) by means of the method of Lagrange multipliers [12], as shown in Eq. (53) below. The transcendental equation resulting from Eq. (53) does not have multiple roots, and enables all the amplitude ratios to be determined. About half the roots coincide in frequency very closely with the double roots obtained from Eq. (48) and are retained and the remaining roots are spurious roots introduced by the constraint condition and are ignored.

In accordance with the foregoing discussion, the constraint condition is written as

$$\lambda_d \int_{R_i}^{R_o} u_r^{(0)} \mathrm{d}r = 0, \quad \text{at } \theta = -\Theta, \tag{52}$$

where λ_d is a Lagrange multiplier, which may be varied freely.

The substitution of the variation of the constraint condition (52) into Eq. (48) along with the constitutive equations (13) and (14) and the introduction of the dimensionless quantities defined in Eqs. (23)–(25) yields

$$\begin{aligned}
&\int_{-\pi/2}^{\pi/2} \Bigg[\Bigg[\Bigg\{ \frac{1}{(\tilde{r}+\bar{r}_0)} \left(\frac{\partial u_r^{(0)}}{\partial \theta} - u_\theta^{(0)} \right) + \frac{\partial u_\theta^{(0)}}{\partial \tilde{r}} \Bigg\} \delta u_r^{(0)} + \bar{c}_{11}^* \Bigg\{ \hat{v} \frac{\partial u_r^{(0)}}{\partial \tilde{r}} + \frac{R}{(\tilde{r}+\bar{r}_0)} \left(\frac{\partial u_\theta^{(0)}}{\partial \theta} + u_r^{(0)} \right) \Bigg\} \delta u_\theta^{(0)} \Bigg]_{\theta=\Theta} \\
&\quad + \Bigg[u_r^{(0)} \delta \Bigg\{ \frac{1}{(\tilde{r}+\bar{r}_0)} \left(\frac{\partial u_r^{(0)}}{\partial \theta} - u_\theta^{(0)} \right) + \frac{\partial u_\theta^{(0)}}{\partial \tilde{r}} \Bigg\} \\
&\quad + \bar{c}_{11}^* u_\theta^{(0)} \delta \Bigg\{ \hat{v} \frac{\partial u_r^{(0)}}{\partial \tilde{r}} + \frac{R}{(\tilde{r}+\bar{r}_0)} \left(\frac{\partial u_\theta^{(0)}}{\partial \theta} + u_r^{(0)} \right) \Bigg\} \Bigg]_{\theta=-\Theta} \Bigg] \mathrm{d}\tilde{r} \\
&\quad + \Bigg[\delta\lambda_d \int_{-\pi/2}^{\pi/2} u_r^{(0)} \, \mathrm{d}\tilde{r} + \lambda_d \delta \int_{-\pi/2}^{\pi/2} u_r^{(0)} \, \mathrm{d}\tilde{r} \Bigg]_{\theta=-\Theta} = 0.
\end{aligned} \tag{53}$$

The introduction of the solution functions (49) and (50) into the variational equation (53) yields a system of $2P+1$ linear homogeneous algebraic equations, which may be written in the matrix form

$$\hat{\mathbf{K}}\hat{\mathbf{X}} = 0, \tag{54}$$

where $\hat{\mathbf{K}}$ is a $(2P+1) \times (2P+1)$ square matrix, $\hat{\mathbf{X}}$ is a $(2P+1)$ unknown column vector, which includes the Lagrange multiplier $\hat{X}_{2P+1} = \lambda_d$.

The vanishing of the determinant of $\hat{\mathbf{K}}$ yields the transcendental equation, which gives the natural frequencies and the mode shapes from the amplitude ratios, which may be determined from any $2P$ of the consistent homogeneous equation (54).

5. Discussion of results

Results are presented for the cantilevered annular sector plate for three different values of $r_0/(2b) = 5/4,\ 5/3$ and $5/2$. Even though the variational equation derived in this work is for the material with polar orthotropic symmetry,[1] the material used in the calculation is for the case of

hexagonal symmetry with the axis of symmetry normal to the plane of the plate. Since the plate is effectively transversely isotropic, it is easy to show that $R = 1$, $c^*_{66} = c^*_{11}(1 - \hat{v})/2$. Thus, the only required material property is the effective Poisson's ratio for the in-plane motion, which is defined in Eq. $(6)_1$.

Through the use of the symbolic package Maple [14], the integration and the matrix manipulation required to treat the characteristic determinant $|\hat{\mathbf{K}}|$ shown in Eq. (54) were performed symbolically and then evaluated numerically using quadruple precision in order to retain complex branches with large imaginary wavenumbers. In the numerical computation, the effective Poisson's ratio of 0.35 was used, as in the case of the study in Part 1, which treats the flexural vibrations of an annular sector plate. The dispersion relations for the three cases are depicted in Fig. 2. In this figure, the dimensionless frequency $\bar{\Omega}$ is plotted against $\Re(\zeta)$ and $\Im(\zeta)$. Here, $\Re(\zeta)$ and $\Im(\zeta)$ represent the real part and the imaginary part of the wavenumber ζ, respectively. As pointed out in earlier work, the inclusion of a complex branch actually means two

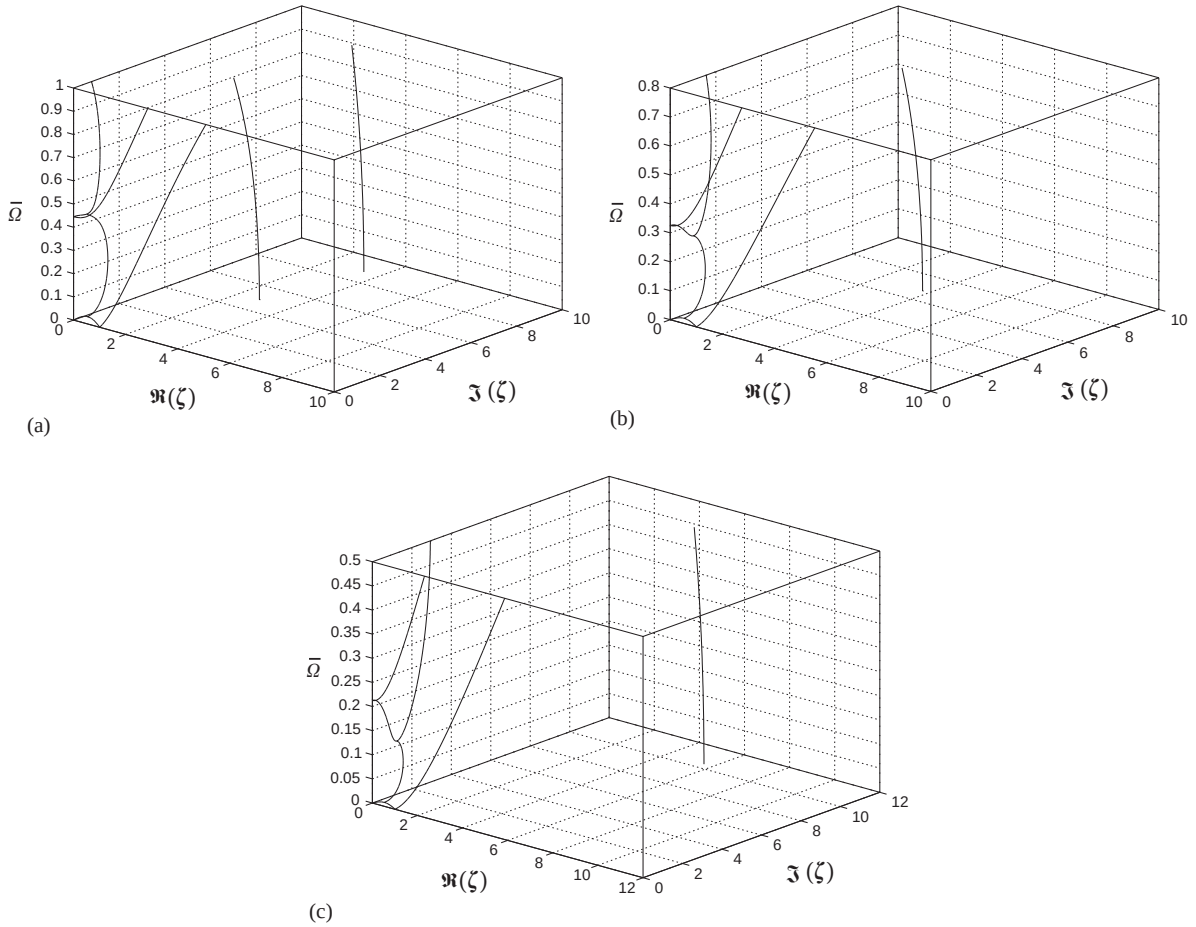

Fig. 2. Dispersion curves for the in-plane motion of the annular sector cantilever plate $\left(r_0 = (R_o + R_i)/2,\ b = (R_o - R_i)/2\right)$: (a) for $r_0/(2b) = 5/4$, (b) for $r_0/(2b) = 5/3$, (c) for $r_0/(2b) = 5/2$.

branches since the complex conjugate pair must be included also. Clearly, the number of complex branches included determines the total number of branches, and hence, the size of the matrix to be treated. Of course, the further inclusion of more dispersion branches will give more accurate results, but it may require additional precision.

The dispersion curves reveal that the nearly straight complex branches move away from the origin, and the most important complex branch, which connects the first real and imaginary branches, gets shorter as the dimensionless radius to the center curve of the annular $\bar{r}_0$ increases. This is a natural consequence of the fact that the wider plate requires more waves to describe the proper modal behavior in this frequency range.

The natural frequencies obtained from the eigenanalysis for the in-plane motion of the cantilevered annular sector plate performed in this work and those obtained from a P3/PATRAN [6] calculation are given in Table 1. As in the work [3] for the case of the out-of-plane motion, around 800 to 1200 quadrilateral shell elements with four nodes were employed for meshing the plates depending upon the aspect ratio of the plate as before, and the subspace iteration method (P3/PATRAN [6]) was adopted for the modal analysis as well. As can be seen from Table 1, in a general sense, the natural frequencies obtained from the analysis presented here are in good

Table 1
Dimensionless natural frequencies for the in-plane motion of the annular sector cantilever plate and their comparison with P3/PATRAN [6] $\left(r_0 = (R_o + R_i)/2,\ b = (R_o - R_i)/2\right)$, N ( ) = Natural frequency $\bar{\Omega}$ (ND) of ( )); C_n (ND) = N (current research) with n dispersion branches included; P (ND) = N (P3/PATRAN)

Mode #	2Θ (rad)											
	$\pi/4$		$\pi/2$		$3\pi/4$		π		$5\pi/4$		$3\pi/2$	
$r_0/(2b) = 5/4$												
1	C_7	0.34589	C_7	0.12088	C_7	0.06227	C_7	0.03948	C_7	0.02863	C_7	0.02284
	P	0.34948	P	0.12180	P	0.06268	P	0.03963	P	0.02876	P	0.02296
2	C_7	0.81921	C_7	0.35191	C_7	0.18076	C_7	0.10556	C_7	0.06810	C_7	0.04785
	P	0.82545	P	0.35417	P	0.18177	P	0.10588	P	0.06840	P	0.04816
	C_7	0.94012	C_7	0.52930	C_7	0.37714	C_7	0.26129	C_7	0.17617	C_7	0.11946
3	P	0.94632	P	0.53125	P	0.37853	P	0.26235	P	0.17708	P	0.11993
$r_0/(2b) = 5/3$												
1	C_5	0.22561	C_5	0.07280	C_5	0.03639	C_5	0.02279	C_5	0.01644	C_5	0.01310
	P	0.22980	P	0.07378	P	0.03661	P	0.02284	P	0.01651	P	0.01314
2	C_5	0.61348	C_5	0.23570	C_5	0.11473	C_5	0.06433	C_5	0.04038	C_5	0.02787
	P	0.61980	P	0.23963	P	0.11595	P	0.06480	P	0.04062	P	0.02797
3	C_5	0.70905	C_5	0.39905	C_5	0.26896	C_5	0.17447	C_5	0.11265	C_5	0.07415
	P	0.71677	P	0.40125	P	0.27125	P	0.17568	P	0.11314	P	0.07449
$r_0/(2b) = 5/2$												
1	C_5	0.11701	C_5	0.03433	C_5	0.01668	C_5	0.01034	C_5	0.00743	C_5	0.00591
	P	0.11852	P	0.03457	P	0.01677	P	0.01035	P	0.00745	P	0.00590
2	C_5	0.38309	C_5	0.12971	C_5	0.05793	C_5	0.03085	C_5	0.01881	C_5	0.01276
	P	0.38790	P	0.13164	P	0.05856	P	0.03101	P	0.01888	P	0.01279
3	C_5	0.47826	C_5	0.25785	C_5	0.15693	C_5	0.09276	C_5	0.05676	C_5	0.03610
	P	0.48253	P	0.25954	P	0.15834	P	0.09323	P	0.05715	P	0.03626

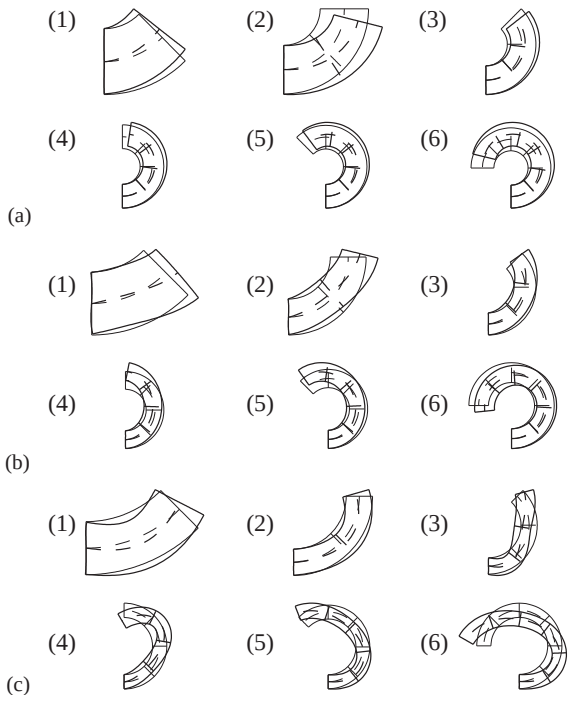

Fig. 3. First six mode shapes for the in-plane motion of the annular sector cantilever plate [(1), …, (6) correspond to $2\Theta = n\pi/4$, $n = 1, \ldots, 6$]: (a) First modes for $r_0/(2b) = 5/4$, (b) second modes for $r_0/(2b) = 5/3$, (c) third modes for $r_0/(2b) = 5/2$.

agreement with those obtained from the P3/PATRAN calculation. The amplitude ratios obtained from Eq. (54) give the mode shapes for some selected cases, which are shown in Fig. 3.

As in the case of the out-of-plane motion of the annular sector plate, as the frequency gets higher, the deviation between the two results gets smaller. The limitation on the number of branches included naturally causes a reduction in accuracy, which should become larger as the width of the annulus gets larger. Of course, this accuracy can readily be improved simply by including more branches, which requires an increase in the computational precision. Since the conditions on the radial edges are only satisfied variationally, the fixed edge does not appear as a straight line in Fig. 3. However, increasing the number of additional branches, not only increases the accuracy of the eigenfrequencies but also causes, the shape of the fixed boundary to approach a straight line.

References

[1] G. Ambati, J.F.W. Bell, J.C.K. Sharp, In-plane vibration of annular rings, *Journal of Sound and Vibration* 47 (2) (1976) 415–432.

[2] T. Irie, G. Yamada, Y. Muramoto, Natural frequencies of in-plane vibration of annular plates, *Journal of Sound and Vibration* 97 (1) (1984) 171–175.

[3] Jongwon Seok, H.F. Tiersten, Free vibrations of annular sector cantilever plates. Part 1: out-of-plane motion, Journal of Sound and Vibration 271 (3–5) (2004) 757–772, this issue.
[4] Jongwon Seok, H.F. Tiersten, H.A. Scarton, Free vibrations of rectangular cantilever plates. Part 1: out-of-plane motion, Journal of Sound and Vibration 271 (1 + 2) (2004) 131–146, this volume.
[5] P.M. Morse, H. Feshback, Methods of Theoretical Physics, McGraw-Hill, New York, 1953, Part I, pp. 530–531.
[6] P3/PATRAN™ User Manual Release 1.2, PDA Engineering-PATRAN Division, 1993.
[7] H.F. Tiersten, Linear Piezoelectric Plate Vibrations, Plenum Press, New York, 1969, Sec. 6.4 (6.44), without the electrical terms and the integral over $S^{(d)}$, since it is for only one region.
[8] R.D. Mindlin, An introduction to the mathematical theory of the vibration of elastic plates, US Army Signal Corps Engineering Laboratory, Fort Monmouth, NJ, 1955, Sec. 3.01.
[9] Jongwon Seok, H.F. Tiersten, H.A. Scarton, Free vibrations of rectangular cantilever plates. Part 2: in-plane motion, Journal of Sound and Vibration 271 (1 + 2) (2004) 147–158, this volume.
[10] F.B. Hildebrand, Methods of Applied Mathematics, 2nd Edition, Prentice-Hall, Englewood Cliffs, NJ, 1965, p. 219, Problem 100.
[11] F.B. Hildebrand, Advanced Calculus for Applications, Prentice-Hall, Englewood Cliffs, NJ, 1976, Sec. 4.4.
[12] R. Courant, D. Hilbert, Methods of Mathematical Physics, Vol. I, Interscience, New York, 1953, Chapter IV, Sec. 9.2.
[13] W.L. Ferrar, Algebra—A Textbook of Determinants, Matrices and Algebraic Forms, Oxford University Press, London, 1941, Chapter VIII.
[14] Maple™ User Manual Release 5, Waterloo Maple Inc., 1997.